THE JOURNAL OF PHYSICAL CHEMISTRY B

Article

pubs.acs.org/JPCB

Multilayers at Interfaces of an Oppositely Charged Polyelectrolyte/Surfactant System Resulting from the Transport of Bulk Aggregates under Gravity

Richard A. Campbell,*[,†] Marianna Yanez Arteta,[‡] Anna Angus-Smyth,[†,§] Tommy Nylander,[‡] and Imre Varga*[,∥]

[†]Institut Laue-Langevin, 6 rue Jules Horowitz, BP 156, 38042 Grenoble Cedex 9, France

[‡]Department of Physical Chemistry, Lund University, P.O. Box 124, S-221 00 Lund, Sweden

[§]Department of Chemistry, Durham University, South Road, DH1 3LE United Kingdom

[∥]Institute of Chemistry, Eötvös Loránd University, Budapest 112, P.O. Box 32, H-1518 Hungary

Supporting Information

ABSTRACT: We show conclusively that multilayers at interfaces of an oppositely charged polyelectrolyte/surfactant system can result from the transport under gravity of bulk aggregates with internal molecular structure. This process was demonstrated by measurements of poly(diallyldimethylammonium chloride)/sodium dodecyl sulfate solutions at the air/liquid and solid/liquid interfaces using neutron reflectometry. In the latter case a novel approach involving the comparison of reflection up versus down measurements provided key evidence. Interfacial multilayers indicated by a strong Bragg peak and clear off-specular scattering are exhibited under three conditions: (1) only for samples in the phase separation region, (2) only for fresh samples where a suspension of bulk aggregates remains in solution, and (3) only when the creaming or sedimentation process occurs in the direction of the interface under examination. This bulk transport mechanism is an alternative route of formation of interfacial multilayers to surface induced self-assembly. The two processes evidently give rise to interfaces with very different structural and rheological properties. Such directionality effects in the formation of nanostructured liquid interfaces may have implications for a broad range of soft matter and biophysical systems containing macromolecules such as synthetic polymers, proteins, or DNA.

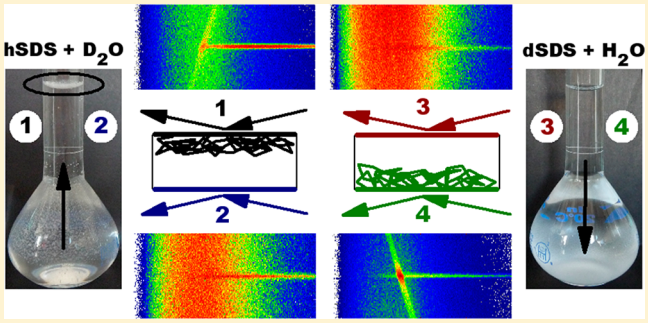

INTRODUCTION

The formation of functionalized interfaces using multilayer assemblies has attracted considerable interest in recent decades both from fundamental[1] and applied[2,3] perspectives. The preparation of electronic and optical devices,[4] sensor surfaces,[5] smart interfaces with the abilities of molecular recognition,[6] and controlled response to external stimuli[7] are just a few promising fields of applications. The most well-known approach for the preparation of controlled multilayer structures is the layer-by-layer deposition technique,[8] which is based on the alternating coating of oppositely charged macroions on an interface but is practically rather laborious. In this respect the formation of self-assembled multilayer structures at interfaces is a promising alternative.

Multilayer formation at air/liquid and solid/liquid interfaces has been reported in a range of aqueous soft matter systems. The most extensively studied category is oppositely charged polyelectrolyte/surfactant (P/S) mixtures, which are important given the massive quantities of synthetic materials used in formulations such as detergents[9] and given that biomacromolecules such as proteins or DNA interact with surfaces in biological processes.[10] It has been discussed in two reviews that some P/S mixtures form multilayers at the air/liquid interface.[11,12] Examples include sodium poly(styrene sulfonate) both with alkyltrimethylammonium bromide surfactants (C_nTABs)[13,14] and a dicationic gemini surfactant,[15] sodium poly(acrylic acid)/C_{12}TAB,[16] and poly(ethylene imine)/sodium dodecyl sulfate (PEI/SDS)[17] and modified PEI/SDS mixtures[18] both at high pH values. Related work has been carried out on short oligomers with oppositely charged surfactants.[19−21] Also, multilayers have been detected at the air/liquid and solid/liquid interfaces for mixtures of comb polymers with surfactants.[22,23]

Although P/S mixtures give the clearest demonstration of multilayers at liquid interfaces, such structures have also been observed for other systems. These include surfactants with

Received: May 10, 2012
Revised: June 12, 2012
Published: June 13, 2012

 © 2012 American Chemical Society

multivalent counterions, such as sodium dodecyl dioxyethylene sulfate with monododecyl dodecaethylene glycol which undergoes a phase transition upon the addition of aluminum ions,[24] and mixtures involving the anionic surfactant sodium 6-dodecylbenzene-4-sulfonate with calcium ions.[25,26] Solutions of aerosol-OT above its critical micelle concentration have been shown to form a lamellar phase at interfaces.[27] Also, multilayers of alternating lipid/protein and solvent have been observed in exogenous lung surfactant mixtures of bovine and porcine origin.[28]

The studies above all used neutron reflectometry (NR) for the detection of multilayers at interfaces. One or more Bragg diffraction peaks in specular reflectivity profiles indicate the presence of repeating structures with scattering contrast perpendicular to the plane of the interface.[29,30] Furthermore, off-specular scattering can result from repeating structures in the direction of the collimated neutron beam.[31,32] In the latter case, a two-dimensional time-of-flight detector image of 2θ with respect to λ, where incoming neutrons of wavelength λ are incident on the sample at a grazing angle of θ, gives a diagonal line.

Despite the wide range of studies that have used NR to detect multilayers at liquid interfaces, further work is required to understand why some soft matter systems exhibit these nanostructured interfaces while others do not.[11,12] A common interpretation is surface induced self-assembly, i.e., amphiphilic components form repeating structures at an interface induced by the presence the surface itself. In contrast, Moglianetti et al. speculated that multilayers of comb polymers and surfactants at the solid/liquid interface may have resulted from adsorption of bulk aggregates with defined internal structure.[23] This interpretation was based on the knowledge that oppositely charged P/S mixtures exhibit associative phase separation close to the charge match point of the components as aggregates flocculate over time due to their lack of colloidal stability.[33−35] Tonigold et al. also discussed the possible connection between interfacial multilayers and the bulk phase behavior. They showed using ellipsometry that there are macroscopic aggregates embedded in molecular adsorption layers of PEI/SDS solutions at pH 10[36] for which interfacial multilayers had been detected previously by NR.[17] Furthermore, Noskov et al. showed using dynamic elasticity measurements that there are microparticles embedded in monolayers of poly(diallyldimethylammonium chloride)/sodium dodecyl sulfate (Pdadmac/SDS) mixtures only in the precipitation region.[37] Even though this work was seemingly unrelated to the issue of interfacial multilayers, we will establish the link in the present paper.

In spite of just a few suggestions of an alternative mechanism to surface induced self-assembly in the creation of interfacial multilayers in soft matter systems, there remained a lack of clear evidence. The primary aims of the present work are to determine the underlying mechanisms that can result in multilayers at the liquid interfaces of a strongly interacting P/S system, and to establish whether the formation of repeating surface structures may be related to a self-assembly process taking place in the bulk rather than one induced by the presence of the surface itself.

The mixture we have chosen for this work is Pdadmac/SDS, which is perhaps a surprising choice to some readers as interfacial multilayers have not previously been observed and the mixture has been categorized as a monolayer system.[11] The system has however attracted particular interest because it exhibits a striking cliff edge peak in its surface tension isotherm.[38] Recently we related the time-dependent production of the peak to the depletion of surface-active material from the bulk due to precipitation[39] and as a consequence to the reduction of the surfactant surface excess at the air/liquid interface.[40] To set the present work into context, the extent and consequence of the precipitation process are demonstrated in Figure 1. After freshly mixed samples with bulk compositions in

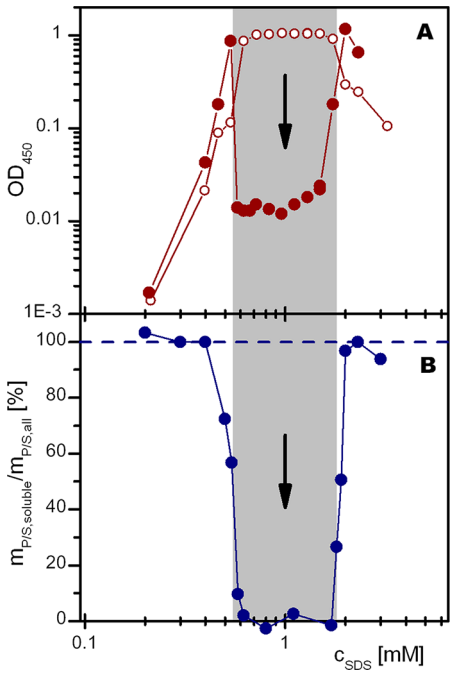

Figure 1. (A) Optical density at 450 nm measured by UV−vis spectroscopy and (B) gravimetric analysis of the P/S complexes remaining soluble or suspended in the bulk solution of the supernatant of aged Pdadmac/SDS solutions left for 3 days to equilibrate (closed symbols); in the former case data from freshly mixed samples are also shown (open symbols). The gray shaded area marks the phase separation region. The samples all contained 100 ppm Pdadmac and 0.1 M NaCl in pure H_2O. Lines are a guide to the eye only. Data are reproduced from ref 40.

the phase separation region have been left to age for 3 days there is a marked reduction in the turbidity of the supernatant (UV−vis measurements; Figure 1A). The lack of colloidal stability of these P/S complexes leads to virtually the total loss of polymer from the liquid phase (gravimetric measurements; Figure 1B). We note that the aged samples in the phase separation region feature a virtually clear supernatant (depleted of material) and white precipitate (containing virtually all of the polymer) that over time has sunk to the bottom of the flasks.

While the link between the slow aggregation process and the depletion of surface-active material from the bulk liquid, and consequently the interface, for this system has been rigorously established, it is also relevant to know how the precipitated particles themselves may affect the interfacial properties. The fact that the precipitate sunk in these samples implies directionality of the bulk aggregate transport as a result of the relative densities of the precipitate and liquid. This prompts us to ask two important questions. First, can we relate the presence of multilayers at interfaces of an oppositely charged P/S mixture to the mean direction of the aggregate transport in the bulk solution? Second, could such directionality effects in

dx.doi.org/10.1021/jp304564x | J. Phys. Chem. B 2012, 116, 7981−7990

the formation of nanostructured interfacial layers affect the physical properties of an interface simply as a result of its given orientation and location in the system?

EXPERIMENTAL SECTION

Materials. Pure H_2O was generated by passing deionized water through a Milli-Q purification system (total organic content = 4 ppb; resistivity =18 mΩ cm). Poly(diallyldimethylammonium chloride) (Pdadmac; 100 000−200 000 g/mol; Aldrich) was purified by dialysis (regenerated cellulose, 12 000−14 000 molecular weight cutoff, Medicell International Ltd.) in pure H_2O to give a stock solution of ∼20 000 ppm (determined by gravimetric analysis) that was free of low molecular weight impurities. Hydrogenous sodium dodecyl sulfate (SDS or hSDS; Sigma; 99.9%) was recrystallized twice in ethanol, and each time the solutions were cooled over several hours to maximize the purity. Deuterated SDS (dSDS; Cambridge Isotopes, 99%) was used as received after checking for contamination with NMR and verifying the purity using surface tension and neutron reflectometry measurements. The solutions made all contained NaCl (Merck; 99.99%). The solvent for neutron reflectometry measurements was either pure H_2O, pure D_2O (Euriso-top, Saclay, France), or a mixture of 8.1% by volume D_2O in H_2O called air contrast matched water (ACMW).

Solution Preparation. The solutions made all comprised 100 mL of 100 ppm Pdadmac at various SDS concentrations in 0.1 M NaCl at 25 °C, except for the gravimetric analysis for which larger samples were required. A standard mixing[36] approach was used to ensure that the mixing of the oppositely charged components took place under reasonably well-defined conditions. These protocols were used to limit the formation of kinetically trapped aggregates as a result of concentration gradients present during mixing.[41] The Pdadmac stock solution produced after the dialysis process was diluted to 200 ppm in 0.1 M NaCl, and for each measurement 50 mL was transferred to a beaker. A stock solution of SDS (∼20 mM) was made fresh and aliquots were transferred by volume to make 50 mL solutions in 0.1 M NaCl in a beaker. To mix each solution, 50 mL of 200 ppm Pdadmac in 0.1 M NaCl and 50 mL of double the intended concentration of SDS in 0.1 M NaCl solution were poured together simultaneously making contact in midair above a 100 mL beaker. The solution was then swirled gently for 3 s to mix the contents of which 30 mL was transferred by a 50-mL glass pipet into a PTFE air/liquid trough or 20 mL was injected in situ through a solid/liquid cell (freshly mixed samples) or the entire solution was poured into a 100-mL volumetric flask and left to age for 3 days (aged samples). In this case care was taken not to agitate any precipitate that had sedimented on the bottom of the flask given that we have demonstrated previously that such agitation to the precipitate can redisperse enough surface-active material to result in a marked effect on the interfacial properties.[39,40]

Air/Liquid Surface Cleaning. The surface of every solution was aspirated for 5 s using a clean pipet attached to a water suction pump. This process served to remove any surface-trapped precipitate and allow time-resolved measurements of adsorption to a fresh surface. We have checked that this procedure does not result in measurable depletion of surface-active material from the bulk by comparing surface tension and ellipsometry data of samples that were aspirated lightly like those in the present work (30% volume loss) with those aspirated heavily (90% volume loss) to observe smaller deviations of the measured values than the experimental error of the measurements.

Hydrophobic Solid Surface Preparation. Silicon crystals of dimensions 50 × 50 × 10 mm were freshly polished on one of the large sides to a roughness of 3 Å (Siltronix, France) and then cleaned in a dilute piranha solution which was maintained at 80 °C for 15 min. The dilute piranha solution comprised a ratio of 5:4:1 of water, sulfuric acid (95−98%, Sigma-Aldrich), and hydrogen peroxide (30% in water, Sigma-Aldrich). After the crystals were rinsed in pure water and dried first under N_2 gas, they were placed in a vacuum desiccator for 1 h. Then 5 mL of methoxydimethyloctylsilane (98%, Sigma-Aldrich) was placed in a glass dish in the center of the desiccator which was left under vacuum for 4 h. The crystals were then rinsed and sonicated for three cycles of ethanol followed by tetrahydrofuran (both analytical reagents). Lastly, the crystals were each dried and mounted in a sealed neutron reflectometry cell consisting of a clamped PTFE trough. The internal volume of each cell of 4 mL was initially filled with ethanol to minimize the formation of air bubbles on the hydrophobic surfaces before they were flushed in situ with degassed water and then exposed to a freshly mixed Pdadmac/SDS solution.

Neutron Reflectometry. The NR measurements were recorded on the time-of-flight horizontal reflectometer FIGARO at the Institut Laue-Langevin (ILL, Grenoble, France).[42] The Bragg peak measurements were recorded using a 20-Å frame overlap mirror and a chopper pair and slit settings that corresponded to a resolution in the momentum transfer of 5%. Off-specular scattering was recorded thanks to the two-dimensional neutron detector. The incidence angle of neutrons on the reflecting surface was 3.8°, a wavelength range of 2−20 Å was recorded, and a wavelength range of 3.4−5.6 Å was used in the peak analysis. The data were reduced into reflectivity with normalization relative to the total reflection of an air/D_2O measurement using the program Cosmos but without data grouping or background subtraction. The Bragg peak area was calculated using a Gaussian fit in the software Origin after a quadratic background, fitted around the peak in the range 0.150−0.165 and 0.185−0.240 $Å^{-1}$, was subtracted from the data. For data with a clear peak the position and full-width-half-maximum were not constrained; for data without a clear peak the parameters were constrained to the mean values derived from data with a clear peak in order to avoid the spurious fitting of false maxima simply due to noise.

UV−vis Spectroscopy. The turbidity of Pdadmac/SDS/NaCl solutions was measured using a Jasco V-630 Spectrophotometer UV−vis spectrometer in a quartz Helma cell with a 1-mm path length for the data in Figure 1, where the optical density (OD) at wavelength 450 nm is given. Each solution was measured within 30 min after its preparation according to the freshly mixed or aged protocols described above. The time-dependent data shown in Figure 3 were measured using a Perkin-Elmer Lambda 2 Spectrophotometer UV−vis spectrometer also in a quartz Helma cell with a 1-mm path length at a fixed wavelength of 400 nm. Since neither the polymer nor the surfactant has an adsorption band above 350 nm, the OD400 and OD450 values have qualitatively the same meaning: the larger the aggregates the larger the OD value. Although the OD400 values will be larger than the OD450 values for equivalent samples, we do not make quantitative comparisons between the two sets of measurements, so they both stand as valid representations of the sample turbidity.

dx.doi.org/10.1021/jp304564x | J. Phys. Chem. B 2012, 116, 7981−7990

Gravimetric Measurements. Pdadmac/SDS/NaCl solutions (300 mL) were prepared in 500 mL glass bottles and were left to age and settle for 3 days. After this time 209 mL of the supernatant was removed with a glass pipet and was transferred into a large glass dish with known mass. It was dried through heating by steam from a water bath then was placed in a vacuum drier at 60 °C for a few hours. The dish was removed warm from the vacuum drier and was placed to cool to ambient temperature in a desiccator (above dry calcium chloride) for 15 min. The heating and drying procedure was repeated (usually for 3 or 4 cycles) until constant mass was reached. The mass of the dry residue was corrected for the amount of salt to show the percentage of polymer and surfactant dissolved or suspended in the solution. This calculation takes the simplest approach of assuming an average stoichiometry of polymer to surfactant in the precipitate of unity; that is, all of the chloride counterions in the polymer are replaced by dodecyl sulfate ions.

RESULTS

NR experiments on soft matter systems commonly exploit isotopic contrast variation in order to determine the structure and composition of material adsorbed or spread at an interface. This approach is based on the assumption that, although the material at the interface scatters neutrons differently depending on the isotopic contrast, the interface is chemically identical for all contrasts measured. However, for systems in which associative phase separation occurs in the bulk, it follows that the isotopic contrast will affect the relative densities of the precipitate and bulk liquid. As phase separation occurs at compositions close to charge neutrality of the bulk complexes for the Pdadmac/SDS system, we start our Results section by highlighting a relevant visual observation. Simply due to density effects, the precipitate in Pdadmac/dSDS/H_2O (or Pdadmac/hSDS/H_2O or Pdadmac/dSDS/D_2O) samples aged for 3 days sank; yet, for Pdadmac/hSDS/D_2O solutions it floated. These directionality effects are demonstrated in photos of samples that had a solution composition corresponding to the charge neutralization point of the bulk complexes,[39] i.e., where the aggregates have the lowest colloidal stability and hence the aggregation process is most efficient, and had been left to age for 3 days (Figure 2). Inhomogenous surface films with a thickness on the order of a few hundred micrometers, each present at only one of the upper or lower surfaces depending on the isotopic contrast, can be clearly identified. We note that anomalies in the interfacial properties of chemically identical P/S solutions due to isotopic contrast variation have been commented for related systems in the literature.[43] Further, it was commented in a recent article that the use of deuterated surfactant in NR measurements could potentially hinder the film-forming potential of a mixture that exhibits phase separation due to density effects.[20] Nevertheless, we are not aware of any investigation that scrutinizes systematically the implications of density effects on the interfacial properties of a P/S system, as is undertaken in the present study.

Given that the density of the aggregates with respect to the bulk liquid determines the direction of creaming or sedimentation, it follows that the rate of the process may also be affected. UV−vis measurements can be used to track the time scale of the creaming/sedimentation process: as the aggregates move either up or down, fewer of them remain suspended in the solution, and the optical density through the center of the sample decreases. Figure 3 shows UV−vis spectroscopy data recorded on the supernatant of samples

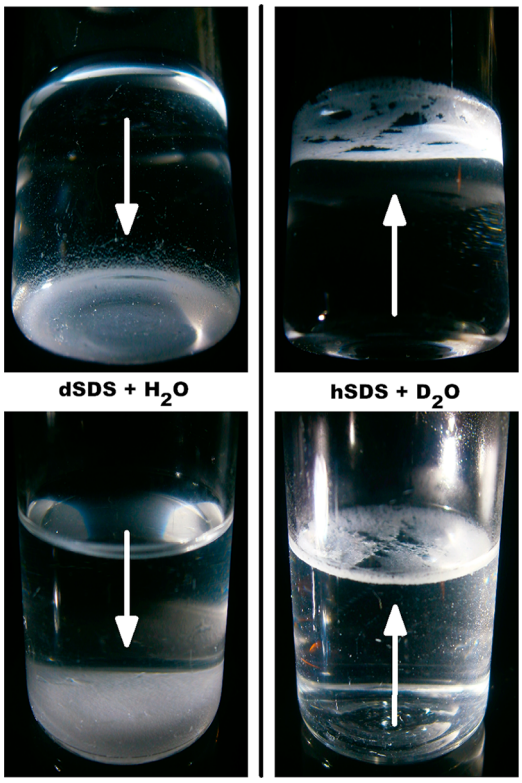

Figure 2. Photos that highlight the different directions of the bulk aggregate transport for aged samples of Pdadmac/dSDS/H_2O (left) and Pdadmac/hSDS/D_2O (right). Perspectives are given both from below the bottom surface (top) and above the top surface (bottom). The samples all contained 100 ppm Pdadmac, 0.82 mM SDS, and 0.1 M NaCl, which matched the point of charge neutralization of the bulk complexes.[39]

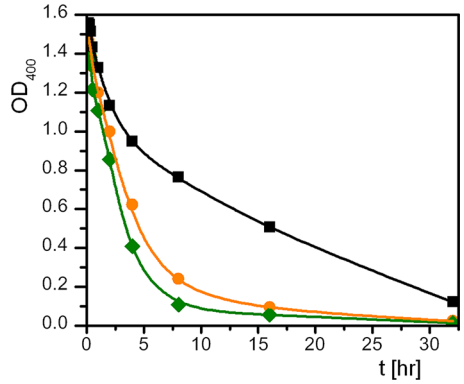

Figure 3. Optical density at 400 nm measured by UV−vis spectroscopy of the supernatant of Pdadmac/SDS samples with time with respect to the isotopic contrast: Pdadmac with hSDS/D_2O (black squares), hSDS/H_2O (orange circles), and dSDS/H_2O (green diamonds). The samples all contained 100 ppm Pdadmac, 0.82 mM SDS, and 0.1 M NaCl. Lines are a guide to the eye only.

prepared in three different isotopic contrasts: Pdadmac with hSDS/D_2O, hSDS/H_2O, and dSDS/H_2O, at bulk composition equivalent to the point of charge neutralization of the bulk complexes.[39] The creaming/sedimentation rates in Figure 3 follow the trend hSDS/D_2O < hSDS/H_2O < dSDS/H_2O. If we compare this trend in the rates of the creaming/sedimentation process to calculated relative densities of the aggregates (ρ_{agg}) and solvent (ρ_{sol}) in each isotopic contrast, $\Delta\rho = \rho_{agg} - \rho_{sol}$

dx.doi.org/10.1021/jp304564x | J. Phys. Chem. B 2012, 116, 7981−7990

(see part 1 of the Supporting Information and Table 1), we can see that the data are in good qualitative agreement: hSDS/D_2O

Table 1. Calculated Densities of Pdadmac/SDS Aggregates and Solvent with respect to the Isotopic Contrast[a]

isotopic contrast	aggregate density, ρ_{agg} (g/cm^3)	solvent density, ρ_{sol} (g/cm^3)	density difference, $\Delta\rho = \rho_{agg} - \rho_{sol}$ (g/cm^3)
Pdadmac/ hSDS/D_2O	1.086	1.099	−0.013 upward
Pdadmac/ hSDS/H_2O	1.037	0.997	0.040 downward
Pdadmac/ dSDS/ ACMW[b]	1.076	1.006	0.070 downward
Pdadmac/ dSDS/H_2O	1.072	0.997	0.075 downward

[a]Derivations may be found in part 1 of the Supporting Information. [b]In addition to the isotopic contrasts shown in Figure 3 calculations are also included for air contrast matched water (ACMW) to highlight its similarity to water in terms of aggregate versus solvent densities.

($\Delta\rho$ = −0.013 g/cm^3, up) < hSDS/H_2O ($\Delta\rho$ = 0.040 g/cm^3, down) < dSDS/H_2O ($\Delta\rho$ = 0.075 g/cm^3, down). It follows that at all time scales until the precipitation process has completed, on the order of days for this system, the rate of sedimentation/creaming will determine the quantity of precipitated particles accumulated at a given horizontal interface at a given time. We will see later that both the direction and rate of the processes are important factors in our understanding of the effects of precipitated particles on the interfacial properties for the Pdadmac/SDS system.

Our previous NR study on the Pdadmac/SDS system was based on the determination of the interfacial composition with respect to the bulk composition and sample history.[40] The interfacial composition was determined by fitting data recorded on a large number of samples prepared in two isotopic contrasts in which the precipitate sank, Pdadmac/dSDS/D_2O and Pdadmac/dSDS/ACMW (air contrast matched water, 91.9% H_2O in D_2O by volume; here we note that there is <1% difference in density between ACMW and H_2O). Measurements were also recorded on samples prepared in the isotopic contrast Pdadmac/hSDS/D_2O, but these data were not used in the determination of the interfacial composition due to the observed creaming of the precipitate (see Figure 2), as this revealed that we could not assume that the structure and composition of the interface were chemically identical to those in the other two isotopic contrasts. Nonetheless we noted the presence of a Bragg peak in some of the data recorded on samples prepared in the Pdadmac/hSDS/D_2O contrast, which initially surprised us given that the system had previously been categorized as a 'Type 2' system exhibiting monolayer adsorption behavior.[11] Here we undertake systematic analysis of the Bragg peak in the data recorded in all three isotopic contrasts in order to determine the conditions under which interfacial multilayer form in this system.

Figure 4A shows the fitted area of the Bragg peak of freshly mixed Pdadmac/SDS solution at the air/liquid interface as a function of the bulk SDS concentration for the three isotopic contrasts. We remind the reader here that freshly mixed samples in the phase separation region are suspensions of bulk aggregates, which either sink or float depending on their density difference with the bulk liquid. For samples at charge neutrality of the bulk complexes,[39] where aggregation is most efficient,

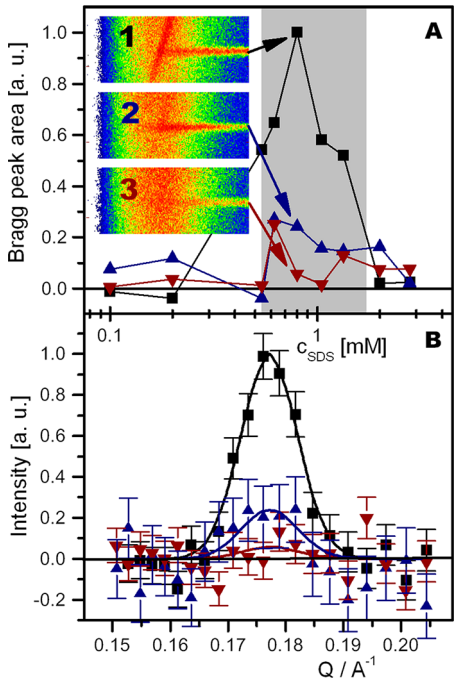

Figure 4. (A) Bragg peak area from NR profiles, fitted on an $R(q)$ scale with a Gaussian function after quadratic baseline subtraction, of Pdadmac/SDS solutions at the air/liquid interface for freshly mixed samples containing Pdadmac with hSDS/D_2O (black squares; 1), dSDS/ACMW (blue triangles; 2), and dSDS/D_2O (red inverted triangles; 3). The corresponding detector images comprise color maps of scattering for reflection angles of ±1.5° (vertical axis) with respect to the wavelength over a range of 1.5−10 Å (horizontal axis). The data are scaled so that the maximum peak area of Pdadmac/hSDS/D_2O equals unity. Lines are a guide to the eye only. (B) Bragg peak in the specular NR profiles at the point of charge neutrality of the bulk complexes (100 ppm Pdadmac, 0.82 mM SDS and 0.1 M NaCl) with Gaussian fits.[39] Data were all recorded with a surface age of 3−5 h. The data are scaled so that the maximum of the Gaussian fit to the Pdadmac/hSDS/D_2O data equals unity. For reference some raw data are later shown in Figure 8.

images of the off-specular scattering are also shown in Figure 4A, and baseline corrected specular reflectivity profiles are displayed in Figure 4B. A sizable Bragg peak occurs only for samples in the phase separation region and only for samples of the isotopic contrast Pdadmac/hSDS/D_2O where the precipitate has a lower density than that of the bulk liquid, i.e., where it creams upward toward the air/liquid interface. The peak position corresponds to a mean repeat d-spacing of 36.0 ± 0.5 Å. Interestingly, bulk studies indicate the formation of long cylinders,[44,45] and the small-angle X-ray scattering data of Sokolov et al.[45] show that they are ordered in a hexagonal phase with a d-spacing of 37 Å, which closely matches our interfacial data. Later in the Discussion section we will demonstrate with simulations of the expected surface structure that the area of the first Bragg peak for Pdadmac/dSDS/ACMW multilayers is in fact expected to be greater than that of chemically identical Pdadmac/hSDS/D_2O samples due to the higher scattering contrast between repeating units within the multilayer. Here we simply note that the discrepancy from this situation in our experimental data is qualitatively consistent with the different directions of aggregate transport in the two isotopic contrasts; that is, for Pdadmac/hSDS/D_2O samples the aggregates were slowly floating toward the interface under examination and for

dx.doi.org/10.1021/jp304564x | J. Phys. Chem. B 2012, 116, 7981−7990

Pdadmac/dSDS/ACMW samples the aggregates were slowly sinking away from it.

As interfacial multilayers were observed for freshly mixed samples only for Pdadmac/hSDS/D_2O in the phase separation region where bulk aggregates were gradually floating up toward the air/water interface, we can now probe the connection between the presence of the surface structure and the effects of slow changes in the bulk phase behavior. The data previously obtained on freshly mixed samples can be compared with data obtained on the supernatant of chemically identical aged samples which are virtually clear as the aggregation and transport processes have already finished (see Figure 1). Figure 5A shows the Bragg peak area with respect to the bulk composition for freshly mixed and the supernatant of aged Pdadmac/hSDS/D_2O samples; for samples at charge neutralization, images of the off-specular scattering are shown in Figure 5A and baseline corrected specular reflectivity profiles are displayed in Figure 5B. It is evident that the interfacial multilayers are essentially now missing for the supernatant of chemically identical samples that are older and depleted of aggregates suspended in the bulk. These results indicate that both the storage time of the sample after mixing and the manner in which it is handled are important parameters in whether interfacial multilayers are detected for the Pdadmac/SDS system.

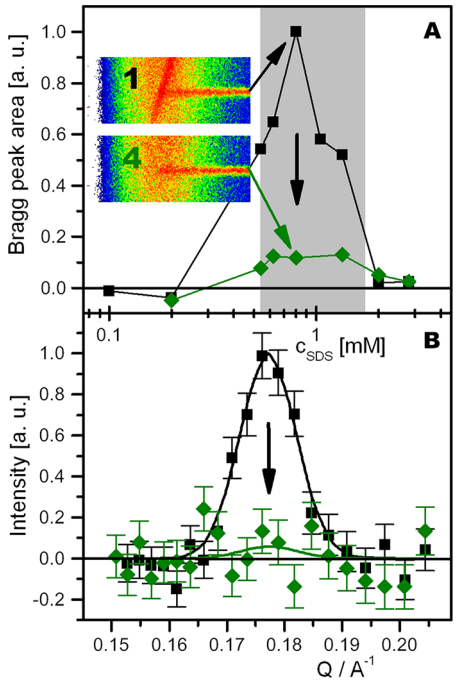

Figure 5. (A) Bragg peak area from NR profiles, fitted on an $R(q)$ scale with a Gaussian function after quadratic baseline subtraction, of Pdadmac/SDS solutions at the air/liquid interface for freshly mixed (black squares; 1) and aged (green diamonds; 4) samples containing Pdadmac with hSDS/D_2O. The corresponding detector images comprise color maps of scattering for reflection angles of ±1.5° (vertical axis) with respect to the wavelength over a range of 1.5−10 Å (horizontal axis). The data are scaled so that the maximum peak area of Pdadmac/hSDS/D_2O equals unity. Lines are a guide to the eye only. (B) Bragg peak in the specular NR profiles at the point of charge neutrality of the bulk complexes with Gaussian fits.[39] Data were all recorded with a surface age of 3−5 h. The data are scaled so that the maximum of the Gaussian fit to the Pdadmac/hSDS/D_2O data equals unity.

Our results at the air/liquid interface can be summarized as follows: a strong Bragg peak and clear off-specular scattering in NR measurements of Pdadmac/SDS solutions are present: (1) only for samples in the phase separation region, (2) only for samples where bulk aggregates float upward to the air/liquid interface rather than sink (i.e., where the bulk aggregates have a lower density than the solvent), and (3) only for freshly mixed samples where there remains a suspension of aggregates in the liquid (i.e., before the bulk has been depleted of material as a result of comprehensive precipitation). These observations are all consistent with the possibility that interfacial multilayers result from the transport of bulk aggregates with ordered internal structure driven to the air/liquid interface by gravity, but they do not provide proof. Ideally we would make parallel NR measurements on a planar air/liquid interface with the air beneath the water, but this cannot be carried out for obvious practical reasons. Nonetheless these results prompted us to look for further evidence to see if this mechanism can explain the presence of interfacial multilayers in the Pdadmac/SDS system.

We formulated a proof-of-principle experiment which would allow us to probe the structure of freshly mixed samples at interfaces located both above and below the bulk solution, to see if we could relate the nature of the formed interfacial layers to the direction of the aggregate transport in the bulk solution: creaming (aggregates moving up) versus sedimentation (aggregates moving down). The simplest way to do so was to examine buried solid/liquid interfaces in sealed sample cells using hydrophobic solid surfaces with two different orientations: interface-above-liquid and interface-below-liquid. Measurements were carried out on solutions with a bulk composition at the point of charge neutrality of the bulk complexes[39] in order to make the aggregation process most efficient in each of two isotopic contrasts: Pdadmac with dSDS/H_2O (maximum particle-to-liquid density difference) and hSDS/D_2O (maximum liquid-to-particle density difference). The FIGARO instrument was again used as it has the unique capability to record data using "reflection up" and "reflection down" configurations in time-of-flight mode and hence allows one easily to measure in sequence samples with different orientations. Table 2 lists the conditions used for this experiment.

If multilayer formation were to result from self-assembly driven by chemical affinity for the surface, then the pairs of experiments involving solutions of the same isotopic composition — i.e., Pdadmac/hSDS/D_2O (samples 1 and 2) and Pdadmac/dSDS/H_2O (samples 3 and 4) — should

Table 2. Summary of Experimental Details for the Four NR Experiments Measured at Hydrophobic Silica/Liquid Interfaces on FIGARO

sample number	isotopic contrast (aggregate transport direction)	sample geometry
1	hSDS/D_2O (moving up)	interface-above-liquid
2	hSDS/D_2O (moving up)	interface-below-liquid
3	dSDS/H_2O (moving down)	interface-above-liquid
4	dSDS/H_2O (moving down)	interface-below-liquid

dx.doi.org/10.1021/jp304564x | J. Phys. Chem. B 2012, 116, 7981−7990

produce equivalent results regardless of the sample orientation. If, however, the direction of the aggregate transport in relation to the surface orientation were a factor then the experiment pairs should be different, and it should be possible to rationalize the magnitude of the surface structure in terms of the density differences between the bulk aggregates and solvent. Note that the smaller number of samples measured here allowed us to record data over a longer period of time and monitor the effects of the sedimentation and creaming processes as the samples got closer to the 3-day aged state for which precipitation has reached completion.

A pronounced Bragg peak and clear off-specular scattering are observed for sample 1 (Pdadmac/hSDS/D_2O; aggregates moving up + interface-above-liquid), and even stronger features are seen for sample 4 (Pdadmac/dSDS/H_2O; aggregate moving down + interface-below-liquid), as shown by the off-specular scattering in Figure 6A and the Bragg peak from the specular reflectivity profiles in Figure 6B. These data reveal the presence of repeating structures both perpendicular to and in the plane of the interface when the measured surface is positioned so that it faces the direction of the bulk aggregate transport. In contrast, crucially, surface repeating structures are totally absent in sample 2 (Pdadmac/hSDS/D_2O; aggregates moving up; interface-below-liquid) and sample 3 (Pdadmac/dSDS/H_2O; aggregate moving down + interface-above-liquid), which have the same bulk chemical *and* isotopic composition as samples 1 and 4, respectively. To our knowledge, these results provide the first conclusive evidence that interfacial multilayers in a polyelectrolyte/surfactant system can form by a mechanism involving the transport under gravity of aggregates with internal molecular structure that had self-assembled in the bulk, rather than by surface induced self-assembly.

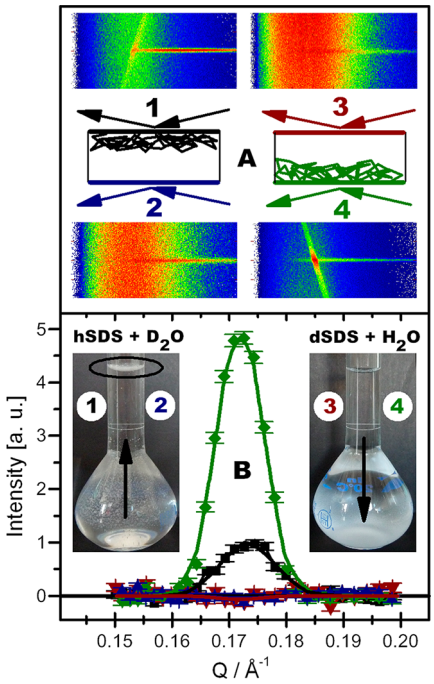

Figure 6. (A) Detector images comprising a color map of scattering for reflection angles of ±1.5° (vertical axis) with respect to the wavelength over a range of 1.5−10 Å (horizontal axis) from NR measurements of Pdadmac/SDS solutions at the hydrophobic solid/liquid interface corresponding to samples 1−4 in Table 2. (B) Bragg peak in the specular NR profiles for black squares (sample 1), blue triangles (sample 2), red inverted triangles (sample 3), and green diamonds (sample 4) each with Gaussian fits, and additional illustrative photos of aged samples of Pdadmac/hSDS/D_2O where the aggregates float (left) and Pdadmac/dSDS/H_2O where the aggregates sink (right). The samples all contained 100 ppm Pdadmac, 0.82 mM SDS, and 0.1 M NaCl, and the data were recorded with a surface age of 27−36 h. The data in panel B are scaled so that the maximum of the Gaussian fit to the Pdadmac/hSDS/D_2O + interface-above-liquid data (sample 1) equals unity. For reference some raw data are later shown in Figure 7.

DISCUSSION

Having demonstrated unequivocally the mechanism of formation of interfacial multilayers for the Pdadmac/SDS system, we will now look in detail at the relative Bragg peak areas for samples of different isotopic contrast at the solid/liquid and air/liquid interfaces to see if they can be rationalized in terms of the underlying physical process. The peak areas are determined by two factors: (1) the difference in neutron scattering length density of the different domains in the multilayered material within the aggregates present at the interface (i.e., the effect of neutron scattering contrast) and (2) the quantity of aggregates accumulated at the interface at the given measurement time as a result of density differences between the bulk aggregates and liquid (i.e., the effects of the direction and rates of sedimentation or creaming as shown in Figures 2 and 3). Both of these factors are affected when we compare samples of different isotopic contrast in the phase separation region.

We will start our analysis with the data recorded at the solid/liquid interface where the key evidence was gathered. Our approach is first to assess the effect of scattering contrast on samples with the same quantity of interfacial material but of different isotopic contrast. This procedure was carried out by simulating the Bragg peak for a given amount of interfacial material for the Pdadmac/hSDS/D_2O + interface-above-liquid data, and then updating the simulation simply by modifying the scattering length densities and level of background scattering for the Pdadmac/dSDS/H_2O + interface-below-liquid data while keeping the quantity of interfacial material constant. Any discrepancy between the simulated and measured peak areas in the latter case can then be rationalized in terms of the effects of the direction or rates of sedimentation or creaming. Later we will adopt the same approach for a comparison of the Pdadmac/hSDS/D_2O and Pdadmac/dSDS/ACMW data at the air/liquid interface.

The presence of interfacial Pdadmac/SDS multilayers was modeled as aggregates in the hexagonal phase[44,45] approximated to stratified polymer-rich and surfactant-rich slabs. Table 3 lists the calculated scattering length densities and layer thicknesses used in the simulations; a detailed description of the approach used and assumptions made may be found in part 2 of the Supporting Information. Note that the single quantity required from each simulation was the ratio of the Bragg peak areas for samples of different isotopic contrast that had the same amount of interfacial material, and this ratio was found to be minimally affected by the interplay between the number of repeating units and the coverage of the multilayer, by the underlying properties of the molecular adsorption layer, and by the slab boundaries used in the multilayer model.

Figure 7 compares the Bragg peak data recorded at the solid/liquid interface for Pdadmac/hSDS/D_2O + interface-above-liquid (sample 1) and Pdadmac/dSDS/H_2O + interface-below-liquid (sample 4) with data simulated for two chemically

dx.doi.org/10.1021/jp304564x | J. Phys. Chem. B 2012, 116, 7981−7990

Table 3. Scattering Length Densities and Layer Thickness for the Slabs Used in the Multilayer Simulations of Hexagonal Phase Pdadmac/SDS Aggregates[a]

isotopic contrast	scattering length density (× 10^{-6} Å^{-2}) of slab A[b] with thickness 24.0 Å	scattering length density (× 10^{-6} Å^{-2}) of slab B[b] with thickness 12.0 Å
Pdadmac/hSDS/D_2O	2.40	4.69
Pdadmac/dSDS/ACMW	3.41	0.27
Pdadmac/dSDS/H_2O	3.20	−0.12

[a]See part 2 of the Supporting Information. [b]Slab A contains the surfactant alkyl chains while slab B is polar according to boundaries shown in Figure ESI1 (see the Supporting Information).

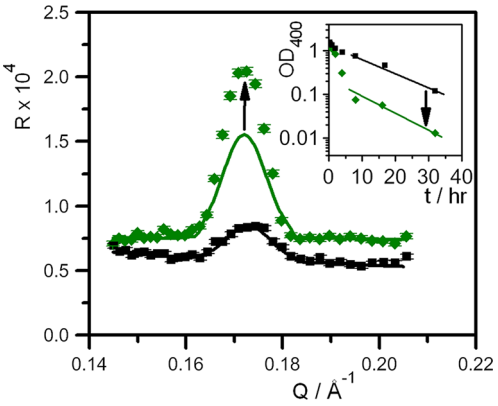

Figure 7. NR Bragg peak for hSDS/D_2O interface-above-liquid (black squares) and Pdadmac/dSDS/H_2O interface-below-liquid (green diamonds) at the solid/liquid interface reproduced from Figure 6 but without background subtraction and multilayer simulations based on the assumption of chemically identical interfaces. The discrepancy between the different ratios of peak areas between the different experiments is qualitatively consistent with the different creaming and sedimentation rates for the two isotopic contrasts calculated in Table 1. The optical density data in the inset, reproduced from Figure 3, indicate the greater quantity of precipitate that is present at the interface for Pdadmac/dSDS/H_2O compared with Pdadmac/hSDS/D_2O.

identical structures, i.e., with the same amount of interfacial material. The ratio of simulated Bragg peak areas for Pdadmac/dSDS/H_2O + interface-below-liquid with respect to Pdadmac/hSDS/D_2O + interface-above-liquid is 3.0. The ratio measured experimentally however is 4.9. This discrepancy by a factor of 1.6 between the experimental and simulated data (see arrow in Figure 7) shows that the difference in Bragg peak areas measured for samples 1 and 4 cannot be accounted for by the effects of the different isotopic contrast alone. To explain this discrepancy we now consider the second contribution to the measured peak area: the relative creaming/sedimentation rates for different isotopic contrasts which result in different quantities of aggregates present at a given horizontal interface at a given time. We recall from above that the rate of aggregate transport of Pdadmac/dSDS/H_2O (down) > Pdadmac/hSDS/D_2O (up); the relevant optical density data from Figure 3 are repeated in the inset of Figure 7 for convenience. The difference in creaming/sedimentation rate for the two samples is qualitatively consistent with the difference in the measured Bragg peak areas for these two systems in relation to the multilayer simulations. While further investigations would be required to probe this link quantitatively, it is clear that the remaining discrepancy in the relative peak areas measured in Pdadmac/hSDS/D_2O + interface-above-liquid (sample 1) and Pdadmac/dSDS/H_2O + interface-below-liquid (sample 4) after correction for the relative scattering contrasts is in line with the different quantities of aggregates present at the interface due to the higher sedimentation rate for Pdadmac/dSDS/H_2O than the creaming rate for Pdadmac/hSDS/D_2O.

Having rationalized the relative Bragg peak areas at the solid/liquid interface in terms of the underlying process in the system, the transport of aggregates in a given direction at a given rate as a result of bulk phase separation, we can now return to the data recorded at the air/liquid interface in Figure 4. We recall that when the probed interface (air/liquid or solid/liquid) is located above the bulk liquid for the Pdadmac/SDS system interfacial multilayers are detected only in the phase separation region where density effects result in the upward transport of structured bulk aggregates. It follows therefore that the same underlying bulk transport mechanism is responsible for the multilayers detected at both the solid/liquid and air/liquid interfaces. We will now see if we can rationalize the relative Bragg peak areas for the different isotopic contrasts measured at the air/liquid interface resulting from the presence of hexagonal phase aggregates using the same approach as above.

Figure 8 compares the experimental Bragg peak data recorded at the air/liquid interface for the Pdadmac/hSDS/

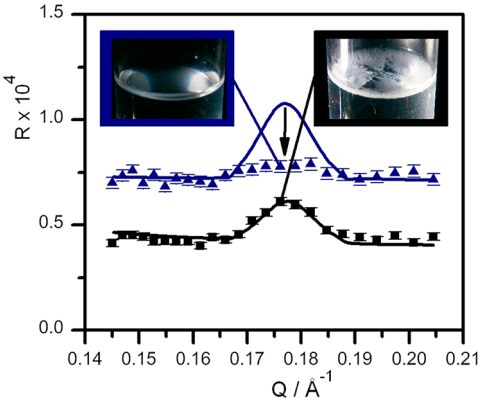

Figure 8. NR Bragg peaks for Pdadmac/dSDS/ACMW (blue triangles) and Pdadmac/hSDS/D_2O (black squares) at the air/liquid interface reproduced from Figure 4 but without background subtraction and multilayer simulations based on the assumption of chemically identical interfaces. The discrepancy between the different ratios of peak areas between the different experiments is more pronounced for this case and can be rationalized by the different directions of the bulk aggregate transport. The photos in the inset, reproduced from Figure 2, show clearly the much greater quantity of precipitate that is present at the interface for Pdadmac/hSDS/D_2O (right) compared with Pdadmac/dSDS/H_2O (left).

D_2O and Pdadmac/dSDS/ACMW contrasts with data simulated for two chemically identical structures; like in the approach used above, the model was refined so that the simulated peak matched the Pdadmac/hSDS/D_2O data and then the appropriate parameters were updated for the Pdadmac/dSDS/ACMW data. The Bragg peak from the latter contrast is expected from the simulations of chemically identical

dx.doi.org/10.1021/jp304564x | J. Phys. Chem. B 2012, 116, 7981−7990

interfaces to be larger by a factor of 1.8; yet, in the measured experimental data it is smaller by a factor of 4.1. In this case the discrepancy by a factor of 7.4 (see arrow in Figure 8) cannot be explained by different mass transport rates: the more extreme mismatch is due to the different directions of the sedimentation or creaming processes. To put it plainly, only a negligible amount of structured material is detected at the air/water interface for Pdadmac/dSDS/ACMW because the air was located above the liquid and the aggregates sank. Although the Bragg peak intensity was not zero in the latter case, we suggest that this may be due to the adsorption of some aggregates to the free-standing interface by Brownian motion. Evidently this effect is minor for this system compared with the process that is driven by gravity as a result of bulk phase separation.

The photos in the inset of Figure 8 remind us that mesostructured Pdadmac/SDS films become macroscopic and are inhomogeneous. The images suggest that creamed or sedimented microparticles may remain largely intact at the interface rather than reorganize to form a uniform film. Such an interpretation would be in line with the findings of Noskov and co-workers,[37] who demonstrated from a drop in the dynamic surface elasticity the presence of microparticles embedded in Pdadmac/SDS adsorption layers in the phase separation region. It follows therefore that the rheological properties of this system may be different to those of a system in which interfacial multilayers form by surface induced self-assembly. We believe that a systematic examination of the connection between the mechanical properties and the underlying mechanism of interfacial multilayer formation in range of other systems that exhibit bulk phase separation would be of great value.

It is clear that both the direction and rate of the bulk aggregate transport for samples in the phase separation region are key factors in the production of interfacial multilayers for the oppositely charged polyelectrolyte/surfactant system studied. It may be intriguing to consider these findings in the context of the interfacial properties of a hanging droplet, where the air is located principally to the sides and beneath the bulk liquid and not above the bulk liquid as for a free liquid surface. There could be very different structural and mechanical properties in the two cases due to the location of the interface with respect to the direction of the earth's gravitational field. Additional factors that affect the formation of interfacial multilayers for the Pdadmac/SDS system include the age of the sample and hence the quantity of bulk aggregates that remain suspended in solution at a given time, slowly traveling in a specific direction toward a horizontal interface. We may also infer that the changing film thickness, and therefore the intensity of diffraction patterns that reveal interfacial multilayers in neutron reflectometry measurements, depend not only on the orientation of the interface under examination but also the specific height of liquid that is located above or below it.

In summary, through systematic examinations of the surface structure of Pdadmac/SDS samples with respect to the bulk composition, isotopic contrast, sample age, interface type and interface orientation, we have shown that without exception the presence of interfacial multilayers can be rationalized in terms of dynamic changes in the bulk phase behavior.

CONCLUSIONS AND OUTLOOK

We have demonstrated that the underlying physical mechanism that results in interfacial multilayers for the Pdadmac/SDS system is the transport under gravity of bulk aggregates with internal structure as a result of their density difference compared with the bulk liquid. This process clearly gives rise to interfaces of very different structure and rheological properties to those of a multilayer formed due to surface induced self-assembly. Also, although it is most intuitive to consider an air/liquid interface with air above a flat liquid surface, this is not the situation in droplets and foams; hence, the directionality effects outlined in this work may influence the surface properties of a range of synthetic and biological macromolecule/surfactant systems including those which involve proteins or DNA in a range of applications. From a technological perspective, it may even be possible to apply the findings of this study to the production of devices coated in nanostructured material on one side but not the other as a result of a bulk self-assembly and gravity-driven transport mechanism.

Our findings indicate the need for future investigations of the physical properties of macroscopic surface films created by oppositely charged polyelectrolyte/surfactant mixtures in the phase separation region. Studies of systems both during the film formation process and after the precipitation and bulk aggregates transport processes have reached completion may help improve our understanding of the dynamic and static behavior of a range of systems which experience bulk phase separation. The application of complementary techniques to examine changes in the film thickness (ellipsometry), lateral morphology (Brewster angle microscopy) and rheological properties (dynamic techniques such as oscillating drop or barrier) could provide additional insight into the nature of the underlying physical processes. Moreover, we conclude that it is important to distinguish which mechanism, transport under gravity of bulk aggregates with internal structure or self-assembly induced by the presence of the surface, is responsible for the presence of interfacial multilayers when detected in soft matter systems. The new neutron reflectometer FIGARO at the ILL, with the ability to inverse the orientation of a buried reflecting interface, has been demonstrated as ideally suited for this purpose.

ASSOCIATED CONTENT

Supporting Information

Density calculations and multilayer simulations. This material is available free of charge via the Internet at http://pubs.acs.org.

AUTHOR INFORMATION

Corresponding Author

*E-mail: campbell@ill.eu; imo@chem.elte.hu.

Notes

The authors declare no competing financial interest.

ACKNOWLEDGMENTS

This work was supported within the 7th European Community RTD Framework Program by the European Reintegration Grant PE-NANOCOMPLEXES (PERG02-GA-2007-2249), the Hungarian Scientific Research Fund OTKA H-07A 74230, the Swedish Foundation for Strategic Research, and the Linnaeus grant "Organizing Molecular Matter" (OMM). I.V. is a Bolyai János fellow of the Hungarian Academy of Sciences which is gratefully acknowledged. We thank the ILL for beam time on FIGARO and the studentship funding for AAS. We also thank Bob Cubitt and Erik Watkins for helpful discussions and Kriszta Sebestyen for assistance with

gravimetric measurements in Figure 1B and UV−vis spectroscopy measurements in Figure 3.

REFERENCES

(1) v. Klitzing, R. *Phys. Chem. Chem. Phys.* **2006**, *8*, 5012−5033.
(2) Nalwa, H. S. *Handbook of Polyelectrolytes and their Applications*, 1st ed.; American Scientific Publishers: New York, 2002; Vol. *1*.
(3) Zhang, S. *Biological and Biomedical Coatings Handbook*, 1st ed.; CRC Press: Boca Raton, FL, 2011.
(4) Arsenault, A. C.; Halfyard, J.; Wang, Z.; Kitaev, V.; Ozin, G. A.; Manners, I.; Mihi, A.; Míguez, H. *Langmuir* **2005**, *21*, 499−503.
(5) Lutkenhaus, J. L.; Hammond, P. T. *Soft Matter* **2007**, *3*, 804−816.
(6) Laschewsky, A.; Wischerhoff, E.; Denzinger, S.; Ringsdorf, H.; Delcorte, A.; Bertrand, P. *Chem.—Eur. J.* **1997**, *3*, 34−38.
(7) Burke, S. E.; Barrett, C. J. *Pure Appl. Chem.* **2004**, *76*, 1387−1398.
(8) Decher, G. *Science* **1997**, *277*, 1232−1237.
(9) Holmberg, K.; Jönsson, B.; Kronberg, B.; Lindman, B. *Surfactants and Polymers in Aqueous Solution*, 2nd ed.; John Wiley & Sons, Ltd.: New York, 2007.
(10) Veis, A. *Biological Polyelectrolytes*, 1st ed.; Marcel Dekker, Inc.: New York, 1970; Vol. *3*.
(11) Taylor, D. J. F.; Thomas, R. K.; Penfold, J. *Adv. Colloid Interface Sci.* **2007**, *132*, 69−110.
(12) Bain, C. D.; Claesson, P. M.; Langevin, D.; Mészáros, R.; Nylander, T.; Stubenrauch, C.; Titmuss, S.; von Klitzing, R. *Adv. Colloid Interface Sci.* **2010**, *155*, 32−49.
(13) Taylor, D. J. F.; Thomas, R. K.; Penfold, J. *Langmuir* **2002**, *18*, 4748−4757.
(14) Taylor, D. J. F.; Thomas, R. K.; Li, P. X.; Penfold, J. *Langmuir* **2003**, *19*, 3712−3719.
(15) Vongsetskul, T.; Taylor, D. J. F.; Zhang, J.; Li, P. X.; Thomas, R. K.; Penfold, J. *Langmuir* **2009**, *25*, 4027−4035.
(16) Zhang, J.; Thomas, R. K.; Penfold, J. *Soft Matter* **2005**, *1*, 310−318.
(17) Penfold, J.; Tucker, I.; Thomas, R. K.; Zhang, J. *Langmuir* **2005**, *21*, 10061−10073.
(18) Zhang, X. L.; Taylor, D. J. F.; Thomas, R. K.; Penfold, J. *Langmuir* **2011**, *27*, 2601−2612.
(19) Penfold, J.; Thomas, R. K.; Zhang, X. L.; Taylor, D. J. F. *Langmuir* **2009**, *25*, 3972−3980.
(20) Jiang, L. X.; Huang, J. B.; Bahramian, A.; Li, P. X.; Thomas, R. K.; Penfold, J. *Langmuir* **2011**, *28*, 327−338.
(21) Halacheva, S. S.; Penfold, J.; Thomas, R. K.; Webster, J. R. P. *Langmuir* **2012**, *28*, 6336−6347.
(22) Moglianetti, M.; Li, P.; Malet, F. L. G.; Armes, S. P.; Thomas, R. K.; Titmuss, S. *Langmuir* **2008**, *24*, 12892−12898.
(23) Moglianetti, M.; Campbell, R. A.; Nylander, T.; Varga, I.; Mohanty, B.; Claesson, P. M.; Makuška, R.; Titmuss, S. *Soft Matter* **2009**, *5*, 3646−3656.
(24) Petkov, J. T.; Tucker, I.; Penfold, J.; Thomas, R. K.; Petsev, D. N.; Dong, C. C.; Golding, S.; Grillo, I. *Langmuir* **2010**, *26*, 16699−16709.
(25) Tucker, I.; Penfold, J.; Thomas, R. K.; Dong, C. C.; Golding, S.; Gibson, C.; Grillo, I. *Langmuir* **2010**, *26*, 10614−10626.
(26) Tucker, I.; Penfold, J.; Thomas, R. K.; Dong, C. C.; Golding, S.; Gisbon, C.; Grillo, I. *Langmuir* **2011**, *27*, 6674−6682.
(27) Li, Z. X.; Lu, J. R.; Thomas, R. K.; Weller, A.; Penfold, J.; Webster, J. R. P.; Sivia, D. S.; Rennie, A. R. *Langmuir* **2001**, *17*, 5858−5864.
(28) Follows, D.; Tiberg, F.; Thomas, R. K.; Larsson, M. *Biochim. Biophys. Acta* **2007**, *1768*, 228−235.
(29) Li, Z. X.; Lu, J. R.; Thomas, R. K.; Penfold, J. *Faraday Discuss.* **1996**, *104*, 127−138.
(30) Savage, D. E.; Kleiner, J.; Schimke, N.; Phang, Y.-H.; Jankowski, T.; Jacobs, T.; Kariotis, R.; Lagally, M. G. *J. Appl. Phys.* **1991**, *69*, 1411−1424.
(31) Richardson, R. M.; Webster, J. R. P.; Zarbakhsh, A. *J. Appl. Crystallogr.* **1997**, *30*, 943−947.
(32) Saville, P. M.; Gentle, I. R.; White, J. W.; Penfold, J.; Webster, J. R. P. *J. Phys. Chem.* **1994**, *98*, 5935−5942.
(33) Kogej, K.; Skerjanz, J. In *Surfactant Science Series*; Radeva, T., Ed.; Marcell Dekker Inc.: New York, 2001; Vol. *99*, p 793.
(34) Evans, D. F.; Wennerström, H. *The Colloidal Domain: where Physics, Chemistry, Biology, and Technology Meet*, 2nd ed.; Wiley-VCH: New York, 1999.
(35) Bergfeldt, K.; Piculell, L.; Linse, P. *J. Phys. Chem.* **1996**, *100*, 3680−3687.
(36) Tonigold, K.; Varga, I.; Nylander, T.; Campbell, R. A. *Langmuir* **2009**, *25*, 4036−4046.
(37) Noskov, B. A.; Grigoriev, D. O.; Lin, S.-Y.; Loglio, G.; Miller, R. *Langmuir* **2007**, *23*, 9641−9651.
(38) Staples, E.; Tucker, I.; Penfold, J.; Warren, N.; Thomas, R. K. *Langmuir* **2002**, *18*, 5147−5153.
(39) Campbell, R. A.; Angus-Smyth, A.; Arteta, M. Y.; Tonigold, K.; Nylander, T.; Varga, I. *J. Phys. Chem. Lett.* **2010**, *1*, 3021−3026.
(40) Campbell, R. A.; Arteta, M. Y.; Angus-Smyth, A.; Nylander, T.; Varga, I. *J. Phys. Chem. B* **2011**, *115*, 15202−15213.
(41) Mészáros, R.; Thompson, L.; Bos, M.; Varga, I.; Gilányi, T. *Langmuir* **2003**, *19*, 609−615.
(42) Campbell, R. A.; Wacklin, H. P.; Sutton, I.; Cubitt, R.; Fragneto, G. *Eur. Phys. J. Plus* **2011**, *126*, 107.
(43) Taylor, D. J. F.; Thomas, R. K.; Hines, J. D.; Humphreys, K.; Penfold, J. *Langmuir* **2002**, *18*, 9783−9791.
(44) Yeh, F.; Sokolov, E. L.; Walter, T.; Chu, B. *Langmuir* **1998**, *14*, 4350−4358.
(45) Sokolov, E. L.; Yeh, F.; Khokholov, A.; Grinberg, V. Y.; Chu, B. *J. Phys. Chem. B* **1998**, *102*, 7091−7098.